ELSEVIER

Contents lists available at ScienceDirect

Surface & Coatings Technology

journal homepage: www.elsevier.com/locate/surfcoat



Cold gas spraying of titanium on stainless steel to enhance corrosion protection inside proton exchange membrane water electrolyzers*

Tim Sievert ^{a,*}, Sarah Zerressen ^b, Martin Bram ^{a,d}, Andreas Glüsen ^b, Klaus Bender ^c, Olivier Guillon ^{a,e}, Robert Vaßen ^{a,d}

- a Forschungszentrum Jülich, Institute of Energy Materials and Devices (IMD), Materials Synthesis and Processing (IMD-2), Wilhelm-Johnen-Straße 5, 2428 Jülich, Germany
- b Forschungszentrum Jülich, Institute of Energy Technologies (IET), Electrochemical Process Engineering (IET-4), Wilhelm-Johnen-Straße 5, 2428 Jülich, Germany
- ^c Bender GmbH Maschinenbau u. Streckmetallfabrik, Ob. Kaiserstraße 4, 57078 Siegen, Germany
- ^d Ruhr-Universität Bochum, Institute for Materials, Universitätsstraße 150, 44801 Bochum, Germany
- e Jülich Aachen Research Alliance: JARA-Energy, 52425 Jülich, Germany

ARTICLE INFO

Keywords: Cold gas spraying Titanium PEM Electrolyzer Corrosion Porous transport layer

ABSTRACT

In order to meet society's increasing energy needs and at the same time reduce the dependence on fossil fuels, it is essential to expand the production of renewable energies. However, a particular challenge of such energies is the discrepancy between energy production and demand. To bridge this gap, methods are needed to store the energy generated. One possibility is the production of green hydrogen by means of Proton Exchange Membrane Water Electrolysis (PEMWE), which can later be used to generate electricity. Consequently, it is crucial to develop costeffective and resource-conserving manufacturing methods for electrolyzer stacks. In this study, we compare a conventionally used porous transport layer (PTL) on the anode side, which consists of a titanium felt, with a new type of PTL made out of a stainless steel expanded metal coated with titanium. Cold gas spraying (CGS) was selected as the coating process, which, like the production of expanded metals, is highly scalable. In addition, cold gas spraying has the advantage that the deposition can take place under normal atmospheric conditions, as comparatively low gas temperatures prevent titanium from undergoing any phase changes. This study shows that it is possible to coat 130 µm thin expanded metals without deformation or blockage. The microstructure was analyzed using scanning electron microscopy (SEM) and the phase composition was determined through X-ray diffraction (XRD) and energy-dispersive X-ray spectroscopy (EDS). The performance of different PTLs was compared by incorporating them into a proton exchange membrane (PEM) electrolyzer test cell. The newly fabricated PTL reached a current density of 2.6 A/cm² at 2 V, which is only slightly lower than the benchmark value, reached with a full-body titanium felt, of 2.9 A/cm². Compared to the full-body titanium felt, our new titanium-coated stainless steel-based PTL can reduce the amount of titanium needed by 68 %.

1. Introduction

Titanium possesses several desirable properties for various applications. Among other things, titanium has a high strength-to-weight ratio and offers excellent corrosion properties, making it a sought-after material for the electrolyzer industry and other applications [1,2]. Nevertheless, compared to alternative materials such as stainless steel, titanium is expensive in terms of both material and processing costs. Due to its high reactivity with oxygen at elevated temperatures, titanium

processing typically requires a controlled atmosphere, such as during physical vapor deposition [3]. However, cold gas spraying provides a unique manufacturing process that allows the deposition of titanium in ambient atmosphere without significant oxidation of the titanium powder.

Cold gas spraying is a thermal spraying process in which, in contrast to others, the powder particles are not molten before they hit the substrate, as the typical deposition temperatures are of $<1100\,^{\circ}$ C. Instead, the process uses a supersonic gas to accelerate the particles to high

 $^{^{\}star}$ This article is part of a Special issue entitled: '11RIPT' published in Surface & Coatings Technology.

Corresponding author.

E-mail addresses: t.sievert@fz-juelich.de (T. Sievert), s.zerressen@fz-juelich.de (S. Zerressen), m.bram@fz-juelich.de (M. Bram), a.gluesen@fz-juelich.de (A. Glüsen), k.bender@benmetal.de (K. Bender), o.guillon@fz-juelich.de (O. Guillon), r.vassen@fz-juelich.de (R. Vaßen).

velocities. This process is particularly useful for metallic materials, where melting under normal atmospheric conditions, as it is the case in atmospheric plasma spraying, would lead to strong oxidation of the powder. When the accelerated particles hit the substrate, bonding occurs due to the plastic deformation of the powder, which necessitates the material to be ductile [4–8].

In order to successfully apply titanium coatings using cold gas spraying, various parameters must be optimized, such as the gas inlet temperature and pressure and the distance between the nozzle and the substrate. In this study, additional challenges are posed by the fragility of the 130 μm thick expanded metals used as substrates. Expanded metals are mesh-like structures produced by slitting and stretching a metal sheet, and can be seen in both coated and uncoated states in Fig. 3 (a), as well as in the cross section of the coated expanded metal in Fig. 4. Furthermore, the holes within the expanded metals must not be clogged by the coating, as they are crucial for the functionality.

These titanium-coated stainless steel expanded metals will later serve as an essential component within a proton exchange membrane electrolyzer (also known as polymer electrolyte membrane electrolyzer), the so-called porous transport layer. Proton Exchange Membrane Water Electrolysis is an effective method for producing green hydrogen, for the chemical storage of energy [9-12]. PEM electrolyzers offer various advantages over other electrolyzers, such as their low operating temperature, high hydrogen purity [9,11,13] and a rapid response time [14,15], which is needed in order to cope with the fluctuating electricity generated by renewable energy sources. One drawback of this technology is its comparatively high capital cost. This is partly due to the highly corrosive conditions inside the PEM electrolyzer, such as the low pH (<2) at the anode side in contact with the catalyst layer, potentials up to 2 V and operating temperatures between 50 and 80 °C [9,11]. Consequently, many components inside the electrolyzer are made out of titanium and are often coated with precious metals such as platinum [9,11]. For instance, the PTL on the anode side typically comprises a titanium felt or expanded metal, both coated with platinum. The primary function of the PTL on the anode side is to transport water to the membrane and to remove the oxygen produced. Additionally, a high electrical conductivity and low contact resistance are essential for a high performance PTL [12,16-18]. Conventional felt-based PTLs have a number of disadvantages compared to expanded metals when coated via cold gas spraying. These include poorer heat dissipation as a result of thinner fibers and a larger thickness, often leading to severe oxidation. In addition, when coating with CGS, the components must be clamped tightly so as not to be moved by the gas flow. The thinner expanded metal with its thicker strands is more resistant to deformation caused by clamping or the supersonic gas flow. Moreover, many felts have finer pore structures, which are likely to be sealed by the powder, compromising the medium transport. Furthermore, the production of expanded metal is a scalable and cheap industrial process. Therefore, this study intends to coat novel stainless steel-based expanded metal PTLs with titanium, optimizing thermal spraying procedures and lowering the total titanium usage.

2. Methods and materials

2.1. Powder

In this study, commercially available, gas atomized, titanium grade 1 powder from TLS Technik GmbH & Co. Spezialpulver KG was used to

Table 1Particle size distribution of the used titanium powder from TLS Technik GmbH & Co. Spezialpulver KG.

Manufacturer's data	D(10)	D(50)	D(90)	Average
[μm]	[μm]	[μm]	[μm]	[µm]
20-53	21.6	36.6	54.1	35 ± 13

fabricate titanium coatings. Table 1 shows the particle size distribution, measured via laser scattering (LA-950, HORIBA Europe GmbH, Germany). Fig. 1 displays SEM (Zeiss GeminiSEM 450) images of the powder, revealing its spherical morphology.

2.2. Titanium deposition

The titanium coatings were deposited using an Impact Innovations GmbH cold spray system, with a D24 converging-diverging nozzle with an expansion ratio of 5.6. Nitrogen was used as both the propellant and feedstock carrier gas. The deposition gas temperature, measured before the gas reaches the nozzle, was 900 °C with a constant gas pressure of 40 bar. For deposition, a stand-off distance of 100 mm at a 90° angle with a gun traverse speed of 2000 mm/s was chosen. The high traverse speed, as well as the omission of any preheating steps, is necessary to avoid damaging or oxidizing the delicate substrates. The coatings were deposited on thin expanded metals which were formed out of 130 μm thick 1.4404 stainless steel sheets by Bender GmbH Maschinenbau u. Streckmetallfabrik. Prior to coating, the expanded metals were cleaned to remove any residue from the surface and then cut with a sheet metal shear into rectangles of 5 cm \times 5.8 cm, leaving 0.4 cm on the top and bottom of the expanded metals for the sample holder to clamp onto. Only the front of the expanded metal, facing the membrane electrode assembly (MEA), was coated with titanium.

2.3. Sample characterization

To examine the phase composition of titanium coatings sprayed under the mentioned conditions, an additional $25~\text{mm}\times25~\text{mm}\times2~\text{mm}$ stainless steel plate was coated and subsequently analyzed with a Bruker D4 diffractometer using a Cu K α anode in a Bragg-Brentano geometry. In order to analyze the coated expanded metals, first top view images were taken before metallographic cross sections were prepared to examine the microstructure. Images were taken with a Hitachi TM 3000 tabletop SEM using a backscatter detector. EDS Analysis was conducted using an EVO 15 SEM from Zeiss with an Ultim Max 100 detector from Oxford Instruments. The thickness and surface area of the coating were measured using ImageJ.

2.4. Performance characterization

To assess the suitability of a stainless steel expanded metal with a cold gas sprayed titanium layer as a PTL within an PEM electrolyzer, the sample was installed in a laboratory-scale test cell, see Fig. 2.

The cell consists of two of meander flow fields, one on the anode side and one on the cathode side. A catalyst-coated membrane that was produced in-house using a Nafion $^{\text{TM}}$ 117 membrane and catalyst loading of 1.00 \pm 0.14 mg Ir/cm² anode catalyst and 0.24 \pm 0.05 mg Pt/cm² cathode catalyst was used. Commercially available carbon PTLs from Toray (TGP-H-120) with a thickness of 360 μm were used as PTLs on the cathode side.

Before installing, the new anode PTL was coated with platinum on both sides by means of sputtering using a Quorum Q150T ES to reach a platinum loading of 0.06 mg/cm² which leads to a coating thickness of about 37 nm. The platinum coating is necessary to prevent titanium oxidation during operation and thus, an increase in contact resistance leading to a performance drop. After assembly, the cells and the purified water were heated to the operating temperature of 80 °C. Subsequently, the cell voltage was ramped up to 1.7 V and held constant for 15 h. Next, I-V curves were recorded to compare the performances of various PTLs. Each voltage step was held for 5 min, with the last 100 s being used to determine the mean current density for that step. This method was used to compare the performance of four different PTLs, see Table 2. A commercially available 360 μ m thick titanium felt (Bekipor® Titanium, 2GDL10–0.35 from NV Bekaert SA) coated with platinum on both sides (Ti_F_Pt) was used as a benchmark, compare Fig. 7. Additionally, similar

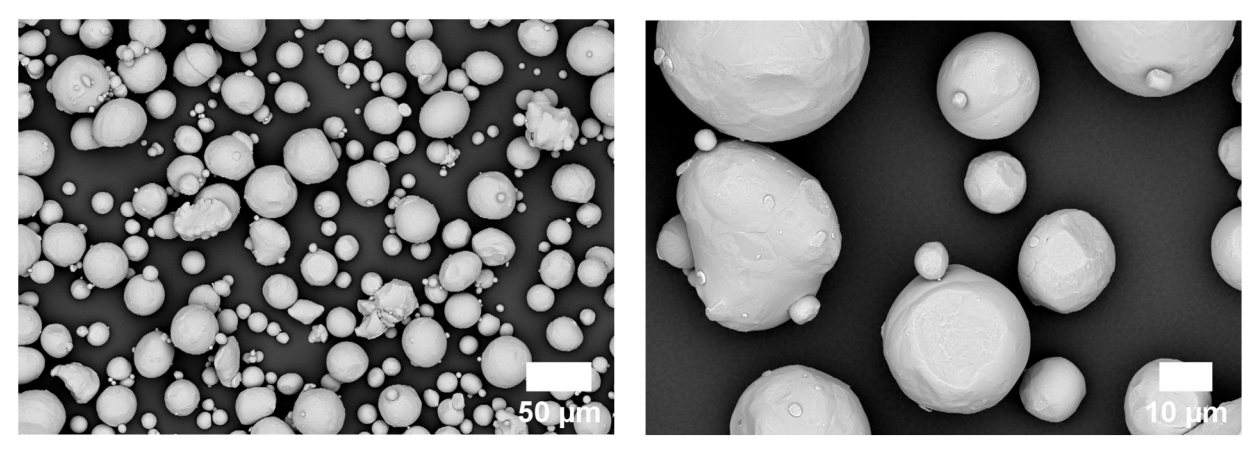


Fig. 1. SEM images using a backscatter detector of the used titanium powder from TLS Technik GmbH & Co. Spezialpulver KG.

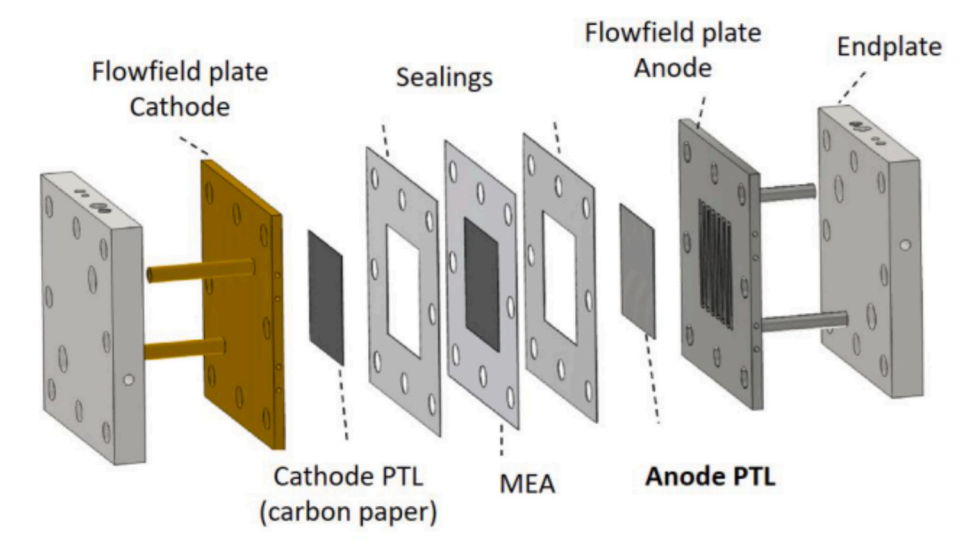


Fig. 2. Illustration of the laboratory sized PEM electrolysis test cell [19].

Table 2Names, buildup, porosity and thickness of the different PTLs tested. All Pt coatings were deposited via sputtering.

Name of PTL	Substrate	Coating 1	Coating 2	Thickness	Porosity
Ti_EM	Ti expanded metal	-	-	125 μm	25 %
Ti_EM_Pt	Ti expanded metal	Pt, both sides	-	125 μm	25 %
Ti_F_Pt	Ti felt	Pt, both sides	-	360 μm	68 %
SS_EM_Ti_Pt	SS expanded metal	Ti, facing MEA	Pt, both sides	168 μm	29 %

expanded metals made of titanium were tested, both with (Ti_EM_Pt) and without (Ti_EM) platinum coating, as well as the newly manufactured stainless steel expanded metal with titanium and platinum coating (SS EM Ti Pt).

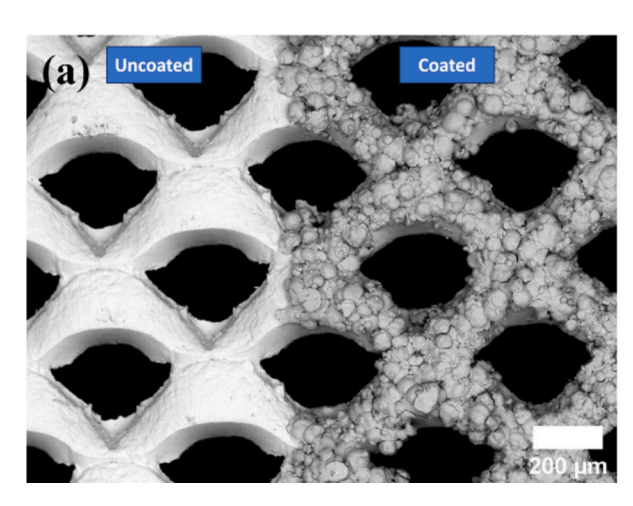
3. Results and discussion

3.1. Scanning Electron microscopy

Fig. 3 shows the top view of the expanded metal that will face the MEA on the anode side of a PEM electrolyzer. Fig. 3(a) shows the surface

of the expanded metal near the edge so that the coated side (right) and the uncoated side (left), which was masked by the clamp and cut off before installation in the electrolyzer, can be seen for comparison. Visibly, the structure as well as the openings of the expanded metal remain intact. Fig. 3(b) shows a higher magnification of the coating, revealing that the deposited titanium particles maintain a spherical shape on the surface, meaning that the titanium particles do not fully flatten upon impact. Thus, the deposition process significantly increases the surface area. Seven different SEM images of cross sections were analyzed, whereby the surface of the uncoated and the coated expanded metal were each measured using ImageJ. Assuming isotropy, this showed that the surface area after coating was increased by 54 % with a standard deviation of 17 %.

The cross sections in Fig. 4 demonstrate that despite the incomplete flattening of the particles, plastic deformation has definitely occurred in the bottom region of the particles, thereby completely covering the substrate. The coating thickness was determined by 60 individual length measurements to be 38 μm with a standard deviation of 16 μm . While this standard deviation is relatively high, it is matching the particle size distribution of the pristine powder, which has an average size of 35 μm with a standard deviation of 13 μm . Therefore, the uneven shape of the coating can be attributed to the titanium particles retaining their shapes. If the current shape of the coating causes issues, using a feedstock powder with a smaller standard deviation as well as reaching higher particles velocities may result in a more uniform coating shape.



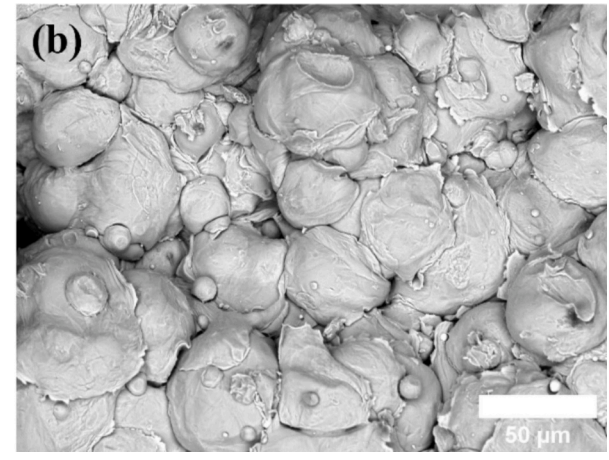
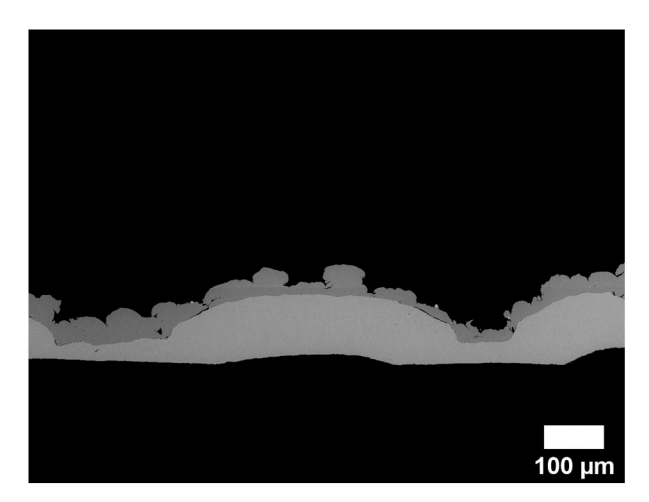


Fig. 3. Top view SEM images of the PTL. (a) Shows the difference between the uncoated state (left, will be cut off before installation in electrolyzer) and the coated state (right, will face the MEA), while (b) shows a higher magnification of the coating.



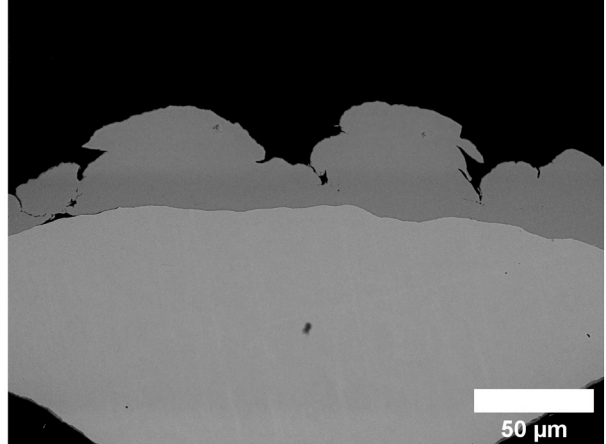


Fig. 4. Cross section SEM images from the titanium-coated stainless steel PTL.

However, it is important to note that an increased surface area, resulting in more three-phase boundaries (catalyst, water, PTL), can enhance performance during operation, as is the case with micro-porous layers [20–22]. To investigate this phenomenon further, manufacturing more PTLs with varying specific surface areas could lead to more insights regarding the surface to performance relation.

Fig. 5 shows the EDS analysis of the cross section of the titanium-coated expanded metal. When reviewing the mapping of the O $k\alpha 1$ signal, it becomes clear that there was no significant oxidation of either the titanium powder or the expanded metal during the deposition. Nevertheless, it should be mentioned that titanium forms a native oxide layer under normal atmosphere in the range of a few nanometers, which is not detectable in the devices used. Overall, the microstructural analysis indicates that the chosen coating parameters successfully achieved full coverage of the expanded metal without clogging its openings or increased oxidation.

3.2. X-ray diffraction

The X-ray diffractogram in Fig. 6 confirms no change of the chemical composition of the titanium powder took place during deposition. The XRD peaks were identified as hexagonal titanium (P63/mmc, $a=b=2.9511\ \mbox{\normalfont\AA}$, $c=4.6843\ \mbox{\normalfont\AA}$). With this result it is possible to conclude that the titanium on the expanded metal also didn't have any major phase changes.

3.3. Reducing titanium usage

This chapter outlines a calculation estimating the potential reduction in titanium consumption by substituting a full-body titanium felt with a stainless steel expanded metal coated with titanium via cold gas spraying.

A commercially available Bekaert titanium felt with a thickness of $360\,\mu m$ (as was used for the benchmark), dimensions of $42\,mm \times 42\,mm$ and a porosity of 68% weighs about 0.915 g. 1 This equates to 0.052 g titanium per cm² of membrane area. In contrast, the titanium coating sprayed with the parameters given in Section 3.2 has a specific weight of 0.009 g/cm², which is a reduction of the specific weight of about 82%. The calculated deposition efficiency, excluding overspray,² for the spray process on the expanded metal was determined to be 55%. This indicates that approximately 0.017 g of titanium per cm² was used to produce the coating. With this adjustment, we calculate that the coating of the stainless steel expanded metal saved about 68% of the titanium that would have been required for the full-body titanium felt.

¹ Calculated using a titanium density of 4.5 g/cm³ [23].

² Here, overspray denotes only the powder deposited next to the substrate, not the powder penetrating the holes of the expended metal. Thus, omitting overspray from the efficiency calculation is appropriate given the smaller size of our test substrates compared to potential industrial applications.

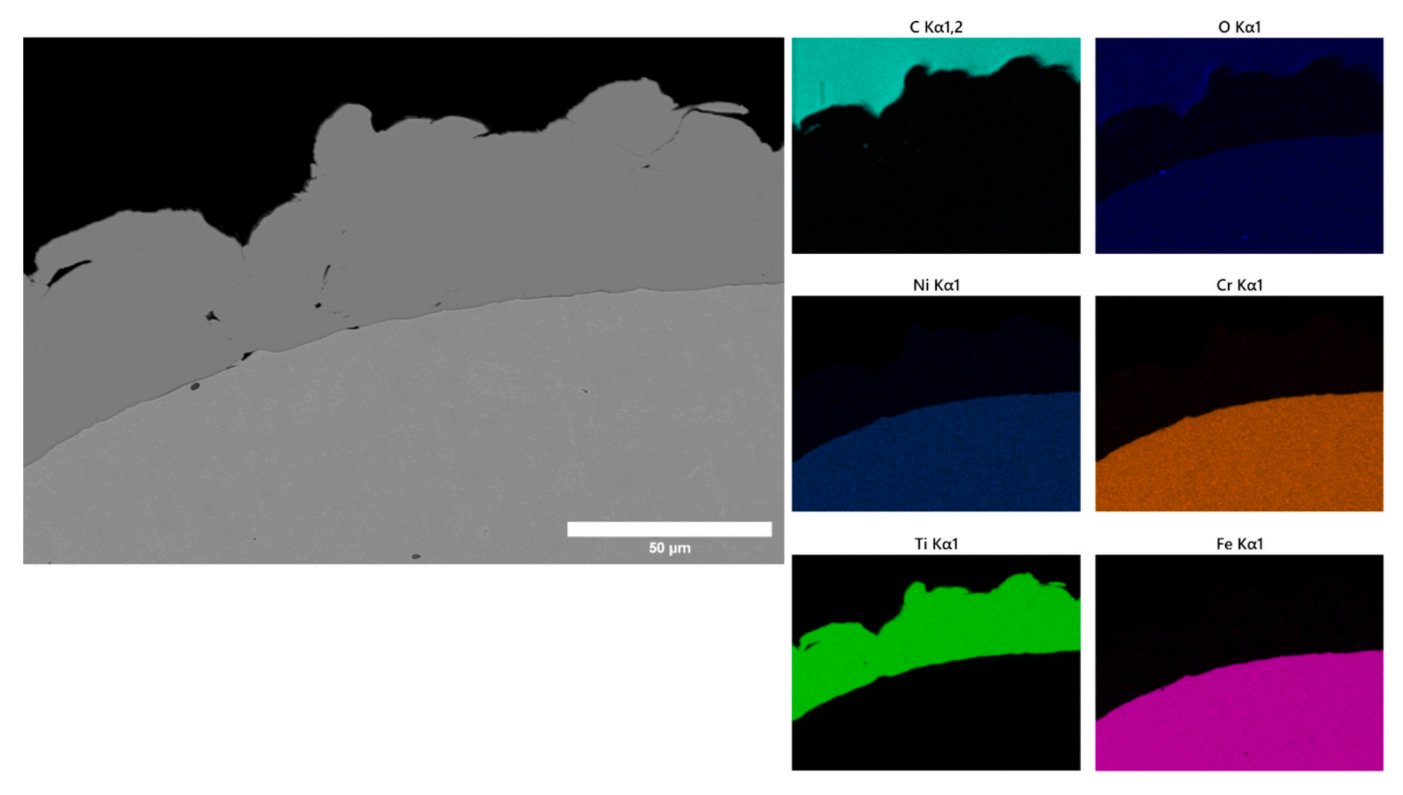


Fig. 5. Cross section SEM image (left) of the titanium-coated stainless steel PTL and EDS mapping of the same spot on the right.

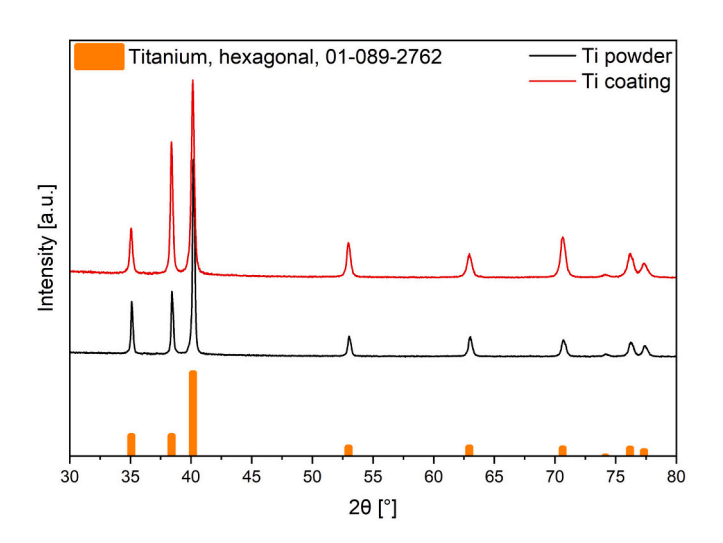


Fig. 6. Normalized diffractogram of titanium deposited by cold gas spraying on a flat stainless-steel substrate (red), the titanium powder (black) and the hexagonal titanium diffraction pattern (orange) used to identify the peaks.

3.4. PEMWE

Fig. 7 displays the recorded I-V curves for various PTLs after the ramp-up stage, as described in chapter 3.4. No data are available on the performance of uncoated stainless steel expanded metals. This is due to the rapid progression of corrosion of the uncoated stainless steel samples during the ramp-up stage, which made it impossible to record I-V curves. The performance of the completely uncoated titanium expanded metal (Ti_EM) is the lowest of the presented I-V curves. The lack of protection against corrosion has presumably caused titanium to oxidize on the surface, thus increasing the contact resistance, resulting in a lower current density (1.3 A/cm² at 2 V). All the platinum coated PTLs performed visibly better as they reach higher current densities. The cell

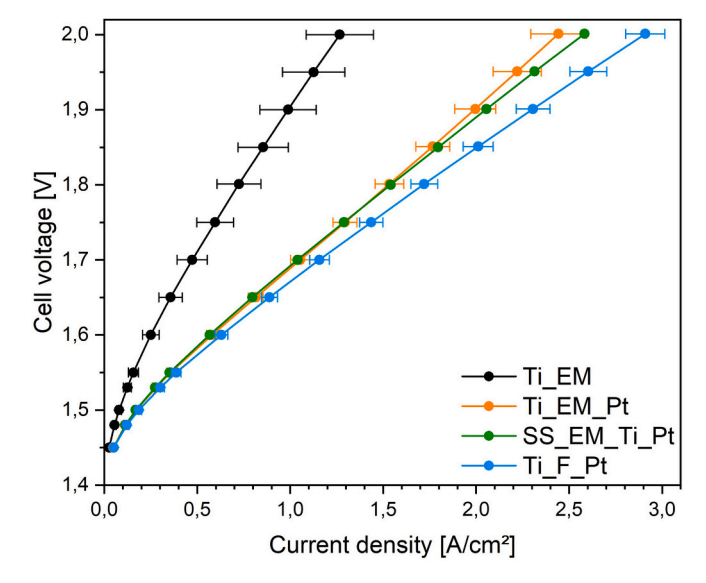


Fig. 7. Current density at different cell voltages after the ramp-up stage for various PTLs.

with the new titanium and platinum coated stainless steel expanded metal (SS_EM_Ti_Pt) exhibits the second highest current density of 2.6 A/cm² at 2 V, which is double the value of the uncoated sample. The cell with platinum coated titanium expanded metal (Ti_EM_Pt) has a slightly lower current density of 2.4 A/cm² at 2 V. Whether this is due to the fact that the titanium expanded metal (Ti_EM_Pt) has a smaller surface area than the stainless steel expanded metal coated with titanium (SS_EM_Ti_Pt) is possible but has not yet been sufficiently investigated. Both of the novel expanded metal-based PTLs are not able to reach the current density of the platinum coated titanium felt (Ti_F_Pt), which reaches a maximum current density of 2.9 A/cm². Nevertheless, SS_EM_Ti_Pt is a

promising candidate that reaches comparable current densities and therefore requires further investigation and optimization.

4. Conclusion

In this study, it was shown that it is possible to use cold gas spraying to successfully coat delicate, thin, porous structures, while avoiding deformation and oxidation of the substrate. This was achieved without significantly oxidizing the titanium powder during deposition. Even though the target current density for PEM electrolyzer cells has not yet been fully reached, the initial tests with the novel PTL are very promising. Thus, coated stainless steel expanded metals, which can be produced in large quantities, appear to be a promising replacement for conventional titanium PTLs, as they can reduce the total amount of titanium required by 68 %. It is important to explore potential benefits of different coating morphologies, for example a higher surface area or different thicknesses, achieved through alternative feedstock powders or deposition parameters to enhance the current density. Further research should also include long-term stability tests in which the current density is monitored over a long period of time and additionally post-mortem analysis of the samples after long operation times to see whether oxidation or coating detachment has occurred.

CRediT authorship contribution statement

Tim Sievert: Visualization, Methodology, Investigation, Data curation, Conceptualization, Writing – review & editing, Writing – original draft. Sarah Zerressen: Investigation, Data curation, Writing – review & editing. Martin Bram: Supervision, Writing – review & editing. Andreas Glüsen: Supervision, Writing – review & editing. Klaus Bender: Resources. Olivier Guillon: Supervision, Writing – review & editing. Robert Vaßen: Supervision, Resources, Project administration, Methodology, Investigation, Funding acquisition, Conceptualization, Writing – review & editing.

Funding

This work was funded by the Federal Ministry of Education and Research (BMBF), Förderkennzeichen 03ZU1115JC. Funding is highly acknowledged.

Declaration of competing interest

The authors declare that they have no known competing financial interests or personal relationships that could have appeared to influence the work reported in this paper.

Acknowledgement

The authors would like to express their gratitude to Karl-Heinz Rauwald (Forschungszentrum Jülich) for his invaluable assistance in conducting the coating experiments. They would also like to thank Dr. Doris Sebold (Forschungszentrum Jülich) for her expertise in performing the SEM analysis of the titanium powder and Andrea Hilgers (Forschungszentrum Jülich) for her contributions to measuring the particle size distribution of the powder. Furthermore, the authors would like to acknowledge the contributions of PD Dr. Georg Mauer (Forschungszentrum Jülich), and Johannes-Christian Schmitt (Forschungszentrum Jülich), who measured the particle velocity.

Data availability

Data will be made available on request.

References

- M.J. Donachie, Titanium: A Technical Guide, 2nd ed., ASM International, 2000 https://doi.org/10.31399/asm.tb.ttg2.9781627082693.
- [2] R.R. Boyer, An overview on the use of titanium in the aerospace industry, Mater. Sci. Eng. A 213 (1–2) (1996) 103–114, https://doi.org/10.1016/0921-5093(96) 10233-1
- [3] W.A. Riehl, C.F. Key, J.B. Gayle, Reactivity of titanium with oxygen, in: George C Marshall Space Flight Cent. Natl. Aeronaut. Space Adm, 1963.
- [4] V.F. Kosarev, S.V. Klinkov, A.P. Alkhimov, A.N. Papyrin, On some aspects of gas dynamics of the cold spray process, J. Therm. Spray Technol. 12 (2) (2003) 265–281, https://doi.org/10.1361/105996303770348384.
- [5] M. Grujicic, C.L. Zhao, C. Tong, W.S. DeRosset, D. Helfritch, Analysis of the impact velocity of powder particles in the cold-gas dynamic-spray process, Mater. Sci. Eng. A 368 (1–2) (2004) 222–230, https://doi.org/10.1016/j.msea.2003.10.312.
- [6] J. Schmitt, J. Fiebig, S. Schrüfer, O. Guillon, R. Vaßen, Adjusting residual stresses during cold spray deposition of IN718, J. Therm. Spray Technol. 33 (1) (2024) 210–220, https://doi.org/10.1007/s11666-023-01673-4.
- [7] H. Assadi, F. Gärtner, T. Stoltenhoff, H. Kreye, Bonding mechanism in cold gas spraying, Acta Mater. 51 (15) (2003) 4379–4394, https://doi.org/10.1016/s1359-6454(03)00274-x.
- [8] T. Klassen, F. Gärtner, T. Schmidt, J.-O. Kliemann, K. Onizawa, K.-R. Donner, H. Gutzmann, K. Binder, H. Kreye, Basic principles and application potentials of cold gas spraying. mater, Werkst 41 (7) (2010) 575–584, https://doi.org/10.1002/ mawe 201000645
- [9] M. Carmo, D.L. Fritz, J. Mergel, D. Stolten, A comprehensive review on PEM water electrolysis, Int. J. Hydrog. Energy 38 (12) (2013) 4901–4934, https://doi.org/ 10.1016/j.ijhydene.2013.01.151.
- [10] S. Stiber, N. Sata, T. Morawietz, S.A. Ansar, T. Jahnke, J.K. Lee, A. Bazylak, A. Fallisch, A.S. Gago, K.A. Friedrich, A high-performance, durable and low-cost proton exchange membrane electrolyser with stainless steel components, Energy Environ. Sci. 15 (1) (2022) 109–122, https://doi.org/10.1039/D1EE02112E.
- [11] M. Prestat, Corrosion of structural components of proton exchange membrane water electrolyzer anodes: a review, J. Power Sources 556 (2023) 232469, https://doi.org/10.1016/j.jpowsour.2022.232469.
- [12] F.J. Hackemüller, E. Borgardt, O. Panchenko, M. Müller, M. Bram, Manufacturing of large-scale titanium-based porous transport layers for polymer electrolyte membrane electrolysis by tape casting, Adv. Eng. Mater. 21 (6) (2019) 1801201, https://doi.org/10.1002/adem.201801201.
- [13] K.W. Ahmed, M.J. Jang, M.G. Park, Z. Chen, M. Fowler, Effect of components and operating conditions on the performance of PEM electrolyzers: a review, Electrochem 3 (4) (2022) 581–612, https://doi.org/10.3390/ electrochem3040040.
- [14] J. Eichman, K. Harrison, M. Peters, Novel Electrolyzer Applications: Providing More Than Just Hydrogen, NREL/TP-5400-61758, 1159377, 2014, https://doi. org/10.2172/1159377. p NREL/TP-5400-61758, 1159377.
- [15] X.-Z. Yuan, N. Shaigan, C. Song, M. Aujla, V. Neburchilov, J.T.H. Kwan, D. P. Wilkinson, A. Bazylak, K. Fatih, The porous transport layer in proton exchange membrane water electrolysis: perspectives on a complex component. sustain, Energy Fuel 6 (8) (2022) 1824–1853, https://doi.org/10.1039/D2SE00260D.
- [16] J.O. Majasan, F. Iacoviello, P.R. Shearing, D.J. Brett, Effect of microstructure of porous transport layer on performance in polymer electrolyte membrane water electrolyser, Energy Procedia 151 (2018) 111–119, https://doi.org/10.1016/j. egypro.2018.09.035.
- [17] A. Bazarah, E.H. Majlan, T. Husaini, A.M. Zainoodin, I. Alshami, J. Goh, M. S. Masdar, Factors influencing the performance and durability of polymer electrolyte membrane water electrolyzer: a review, Int. J. Hydrog. Energy 47 (85) (2022) 35976–35989, https://doi.org/10.1016/j.ijhydene.2022.08.180.
- [18] H. Wakayama, Low-cost porous transport layers for water electrolysis cells with polymer electrolyte membranes, Mater. Res. Express 11 (8) (2024) 085501, https://doi.org/10.1088/2053-1591/ad666e.
- [19] S. Holtwerth, Mechanisches Verhalten von Polymer-Elektrolyt-Membran-Elektrolysezellen und -Stacks (Dissertation), 2022, https://doi.org/10.18154/ RWTH-2023-04311.
- [20] T. Schuler, J.M. Ciccone, B. Krentscher, F. Marone, C. Peter, T.J. Schmidt, F. N. Büchi, Hierarchically structured porous transport layers for polymer electrolyte water electrolysis, Adv. Energy Mater. 10 (2) (2020) 1903216, https://doi.org/10.1002/aenm.201903216.
- [21] P. Lettenmeier, S. Kolb, F. Burggraf, A.S. Gago, K.A. Friedrich, Towards developing a backing layer for proton exchange membrane electrolyzers, J. Power Sources 311 (2016) 153–158, https://doi.org/10.1016/j.jpowsour.2016.01.100.
- [22] J.K. Lee, A. Bazylak, Balancing reactant transport and PTL-CL contact in PEM electrolyzers by optimizing PTL design parameters via stochastic pore network modeling, ECS Trans. 92 (8) (2019) 801–820, https://doi.org/10.1149/ 09208.0801ecst.
- [23] N.N. Greenwood, A. Earnshaw, N.N. Greenwood, Chemie der Elemente, 1. korrigierter Nachdr. d. 1. Aufl, VCH, Weinheim Basel (Schweiz) Cambridge New York, NY, 1990.